

# Simple Model of Membrane Proteins Including Solvent

D. L. Pagan, A. Shiryayev, T. P. Connor, and J. D. Gunton

*Department of Physics, Lehigh University, Bethlehem, P.A. 18015*

## Abstract

We report a numerical simulation for the phase diagram of a simple two dimensional model, similar to one proposed by Noro and Frenkel [J. Chem. Phys. **114**, 2477 (2001)] for membrane proteins, but one that includes the role of the solvent. We first use Gibbs ensemble Monte Carlo simulations to determine the phase behavior of particles interacting via a square-well potential in two dimensions, for various values of the interaction range. A phenomenological model for the solute-solvent interactions is then studied to understand how the fluid-fluid coexistence curve is modified by solute-solvent interactions. It is shown that such a model can yield systems with liquid-liquid phase separation curves that have upper and lower critical points, as well as closed loop phase diagrams, as is the case with the corresponding three dimensional model.

## I. INTRODUCTION

Although there exists no theoretical framework concerning how to optimally grow protein crystals, experimentalists have produced a large number of globular protein crystals suitable for x-ray diffraction. This is evidenced by the large number of crystal structures available in the protein databank<sup>1</sup>. The situation, however, is rather different for the case of membrane proteins, a class of important proteins which are characterized as being attached to a lipid membrane<sup>2</sup>. By comparison, far fewer membrane protein structures are known than for globular proteins, due to the difficulty in crystallizing membrane proteins. It has been shown that membrane proteins can be more easily crystallized if they are forced to interact in a quasi-two dimensional space<sup>3</sup>. Many approaches to crystallizing membrane proteins utilize this procedure. Thus it is of interest to know the general features of the phase behavior of quasi-two-dimensional proteins and to compare these with those for globular proteins.

The phase behavior of globular proteins has been modelled using a colloidal approach. It has been shown<sup>4,5,6,7,8,9,10,11,12</sup> that to a reasonable first approximation these proteins can be modelled using a short-range attractive interaction and a hard-core repulsion. Indirect evidence suggests that membrane proteins also interact via a short-range interaction as well. As a consequence, a generic phase diagram for membrane proteins has been proposed<sup>14</sup> based on a short-range interaction model. In addition, a similar approach<sup>13</sup> has been used to successfully model the phase behavior of the protein Annexin V. However, an important effect that has been largely ignored until recently is the role of the solvent-solute interactions on such phase diagrams. For three-dimensional globular proteins, crystals are grown using a combination of a variety of precipitating agents, including salts and polyethylene glycol. These agents (along with other additives to control such parameters as the pH), are used to fine-tune the interactions between proteins and control the range and strength of interactions between protein particles. Precipitating agents are also important in crystallizing membrane proteins. As a first step toward understanding the role of solvent-solute interactions in protein crystallization, a model was proposed recently<sup>15</sup> for globular proteins interacting via a short-range potential interacting in three dimensions. In that study, it was shown that a variety of phase diagrams could be obtained for different choices of the solute-solvent parameters. In this paper we extend that study to model particles interacting in a quasi two-dimensional plane in the presence of a solvent. We consider the particular case of

particles interacting via a square-well potential, in the absence of solvent, determining the fluid-fluid coexistence curves for several different interaction ranges, using standard Monte Carlo methods. We then obtain the phase diagram for such a system taking into account solvent-solute interactions and show that there are several possible types of phase diagrams, depending on the choice of interaction parameters. Namely, the model can have an upper critical point, a lower critical point, or closed loop phase diagrams, depending on the solvent-solute interactions.

## II. COMPUTATIONAL AND THEORETICAL DETAILS

We use a square well potential to model the attractive interactions between protein particles interacting in a 2D plane. The square well potential is given by

$$V(r) = \begin{cases} \infty, & r < \sigma \\ -\epsilon, & \sigma \leq r < \lambda\sigma \\ 0, & r \geq \lambda\sigma, \end{cases} \quad (1)$$

where the particle diameter,  $\sigma$ , the well-depth,  $\epsilon$ , and  $\lambda$  set the length, energy scale and interaction range, respectively. We consider the three cases  $\lambda = 1.50$ ,  $\lambda = 1.75$  and  $\lambda = 2.0$ . To calculate the fluid-fluid coexistence curves, we employ the Gibbs ensemble Monte Carlo method<sup>16</sup>. This method is well suited to studying such systems away from the critical point and is a standard technique.

As noted in the introduction, membrane proteins are often crystallized in two dimensions (2D) where, as in three dimensions (3D), various solvents are used to promote crystallization. These precipitating agents thus play an important part in the crystallization process. As noted in the introduction, a simple phenomenological model for the role of solvent has been proposed<sup>15</sup>. The multi-component system (i.e., proteins plus solvent) is modelled as a binary system in which the solute particle is much bigger than the solvent. It is also assumed that the effect of the other components are subsumed in the effective solute-solvent interaction.

The total energy of a protein system interacting via a short-range potential can be written as

$$U_0(\vec{r}^N) = \frac{1}{2} \sum_{i \neq j} U_0(|\vec{r}_i - \vec{r}_j|), \quad (2)$$

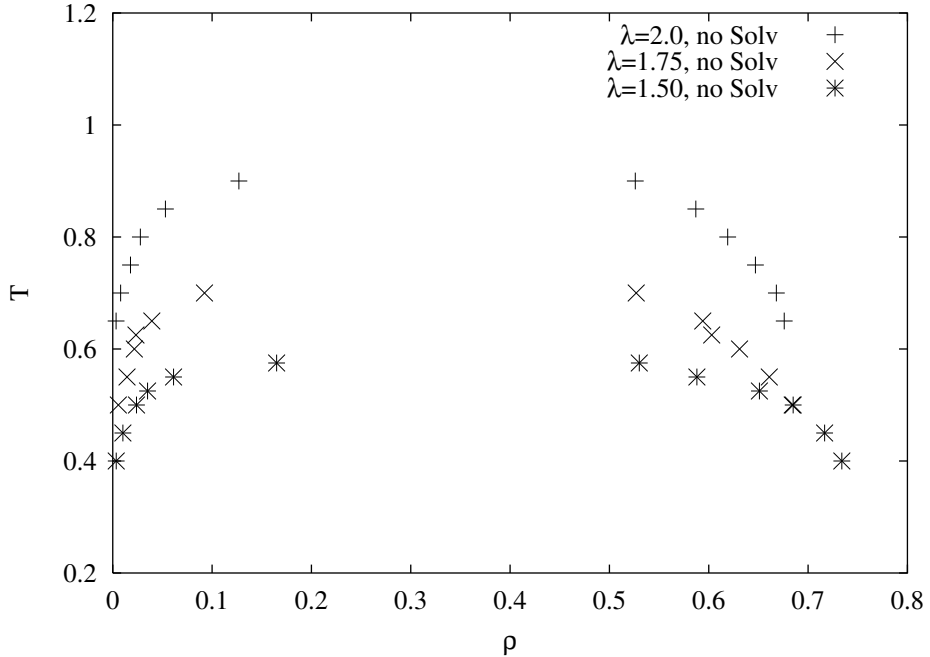


FIG. 1: Fluid fluid coexistence curves for the ranges  $\lambda = 2.0, 1.75$ , and  $1.50$  for the 2D square well model.

where the subscript '0' denotes the potential of the protein in the absence of solvent. The model that incorporates the effect of solvent has a total potential

$$U = U_0 + \sum (\epsilon_w - k_B T \Delta s_w) n_w^{(i)}(\vec{r}^N), \quad (3)$$

where  $n_w^{(i)}$  is the number of water molecules around the  $i^{th}$  particle and  $\epsilon_w$  and  $s_w$  are the interaction energies and entropy of the solvent, respectively. The authors show<sup>15</sup> that this solvent-solute interaction leads to an effective protein-protein square well interaction whose strength is given by  $\tilde{\epsilon} = \epsilon + 2\epsilon_w - 2k_B T \Delta s_w$ . Thus the Boltzmann weighting factor for the system with solvent is the same as the one without solvent, except that  $\tilde{\epsilon}$  replaces  $\epsilon$ . This yields several results for the model with solvent in terms of the behavior of the model without solvent. For example, the phase diagram for the system with solvent-solvent interactions is given by

$$k_B T_{coex} = \frac{(\epsilon_0 + 2\epsilon_w)}{1 + 2\Delta s_w \tau(\rho)} \tau(\rho), \quad (4)$$

where  $\tau(\rho)$  is the functional form of the coexistence curve (denoting two coexisting phases) without solvent. This expression is independent of dimensionality. Similarly, the radial distribution function for the system with solvent-solute interactions is given in terms of such

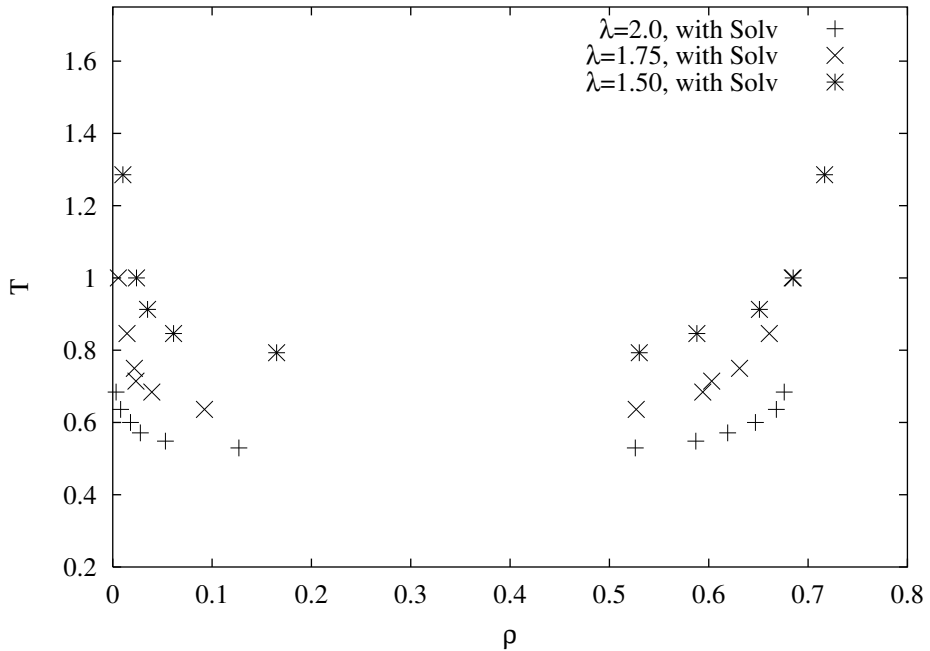


FIG. 2: Fluid fluid coexistence curves for the ranges  $\lambda = 2.0, 1.75$ , and  $1.50$  for the 2D square well model.

interactions by

$$g_s(r) \equiv g_0(r; \tilde{\epsilon}). \quad (5)$$

Correspondingly, the structure factor for the system with solvent-solute interactions is given by

$$S_s(q) = S_0(q; \tilde{\epsilon}). \quad (6)$$

For a complete discussion of the model, the reader is referred to Ref. (15).

We obtained the fluid-fluid coexistence curves of  $N = 250$  particles without solvent via Monte Carlo simulations. We then use eq. (4) to determine the coexistence curves of the particles interacting via eq. (1) that includes the solvent-solute interactions. Equilibration runs lasted 10 million Monte Carlo (MC) steps, production runs lasted 20 million MC steps. Isobaric-isothermal (NPT) Monte Carlo simulations<sup>17</sup> were employed to sample the fluid and solid phases of the 2D system without solvent. For sufficiently low ranges of  $\lambda$ , we observed a tendency for the fluid to crystallize and the solid phase to melt at appropriate pressures, as found in another study<sup>14</sup>. To overcome this difficulty, we employ a biasing parameter which allows us to force the system into either a liquid or solid state. We use the bond-order

parameter<sup>18</sup> defined by

$$Q_{lm} \equiv Y_{lm}(\phi(\vec{r})), \quad (7)$$

where  $Y_{lm}$  are the spherical harmonics. We calculate the bond order parameter<sup>18</sup>,  $Q_6$ , which has a non-zero value for a two dimensional solid and a zero value for the liquid.  $Q_6$  is calculated<sup>18</sup> as

$$Q_l = \left[ \frac{4\pi}{2l+1} \sum_{m=-l}^{m=l} \langle Q_{lm} \rangle^2 \right]^{1/2}. \quad (8)$$

Less than 5% of all configurations are rejected in any simulation of the liquid or solid. Using this order parameter we are able to sample fluid and solid phases and measure the radial distribution function,  $g(r)$ , and the bond-pair correlation function, given by

$$g_6(r) = \langle \psi_6^*(\vec{r}_j) \psi_6(\vec{r}_i) \rangle \quad (9)$$

where the local bond-order parameter  $\psi(\vec{r}_i)$  for particle  $i$  at position  $\vec{r}_i$  is given by

$$\psi_6(\vec{r}_i) = \frac{\sum_k w(r_{ik}) \exp(i6\theta_{ik})}{\sum_k w(r_{ik})}. \quad (10)$$

The summation is over neighboring particles  $k$  of particle  $i$ ;  $\theta_{ik}$  is the angle between the vector  $(\vec{r}_i - \vec{r}_k)$  and a fixed reference axis. The weighting factor  $w$  is used to define nearest neighbors.

### III. RESULTS AND DISCUSSION

The fluid-fluid coexistence curves have been calculated using Gibbs ensemble Monte Carlo. The fluid-fluid coexistence curves for three values of  $\lambda$  are shown in Fig. 1. It is worthwhile to compare these coexistence curves to their 3D counterparts<sup>19</sup>. The critical temperatures in 2D at these  $\lambda$  are relatively close to each other when compared to those in 3D. Also, the critical temperatures are lower than those in 3D. The critical densities are different as well, yet they exhibit the same behavior as their 3D counterparts - the critical density increases with decreasing  $\lambda$ . Below  $\lambda = 1.50$ , we were unable to obtain a fluid-fluid coexistence curve. For particles interacting via a range of attraction of  $\lambda = 1.375$ , we observed that the particles form either a solid or liquid phase. Similar behavior has been

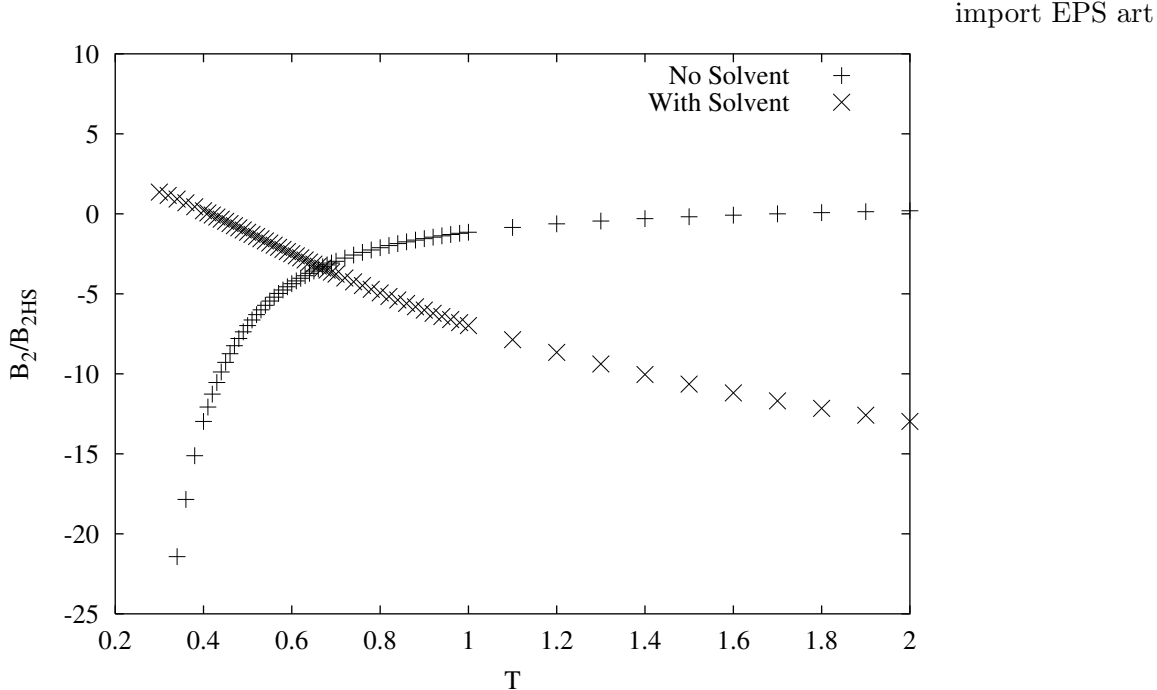


FIG. 3: Second virial coefficient as a function of temperature in the absence and presence of the solvent.

observed for another system of particles interacting via a short-range potential<sup>14</sup> in 2D. In that study, this phenomenon was observed at short-ranges of attraction corresponding to the case where the spinodal curve is metastable with respect to the liquidus-solidus curve, suggesting that the binodal curve is metastable as well. It has been proposed<sup>14</sup> that the free-energy barrier to be overcome is much smaller in 2D than in 3D. Thus, at sufficiently low ranges of interaction, the metastable fluid-fluid coexistence curve cannot be sampled. In analogy with this system, we estimate that the threshold value for metastability lies within the range  $1.375 \leq \lambda \leq 1.50$ .

To obtain the fluid-fluid coexistence curves with solvent we used eq. (4). It has been shown<sup>15</sup> that for appropriate choices of the parameters  $\epsilon_w$  and  $s_w$ , a variety of phase diagrams can be realized. We chose the parameters  $\epsilon_w = -1.0$  and  $s_w = -1.50$  to see how the 2D fluid-fluid coexistence curves are affected in the presence of solvent with these particular interaction parameters. For these values of the parameters, it has been shown<sup>15</sup> for the 3D square well model that the phase diagram at  $\lambda = 1.25$  has a lower critical point, whereas the model in the absence of solute-solvent interaction has an upper critical point. We find a similar behavior in 2D. It remains to be seen, however, if whether membrane proteins (or

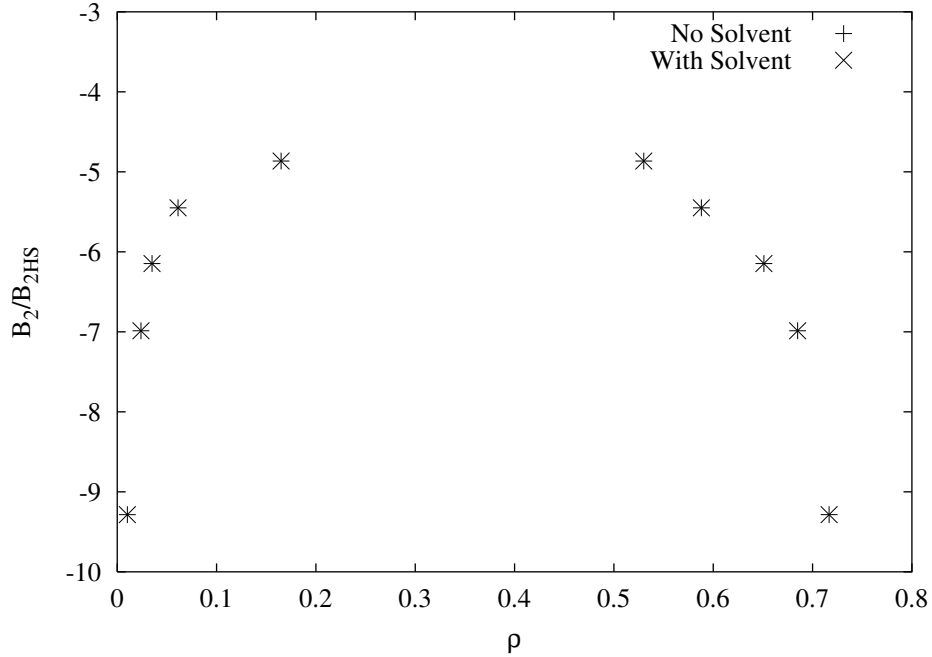


FIG. 4: Second virial coefficient as a function of density in the absence and presence of the solvent.

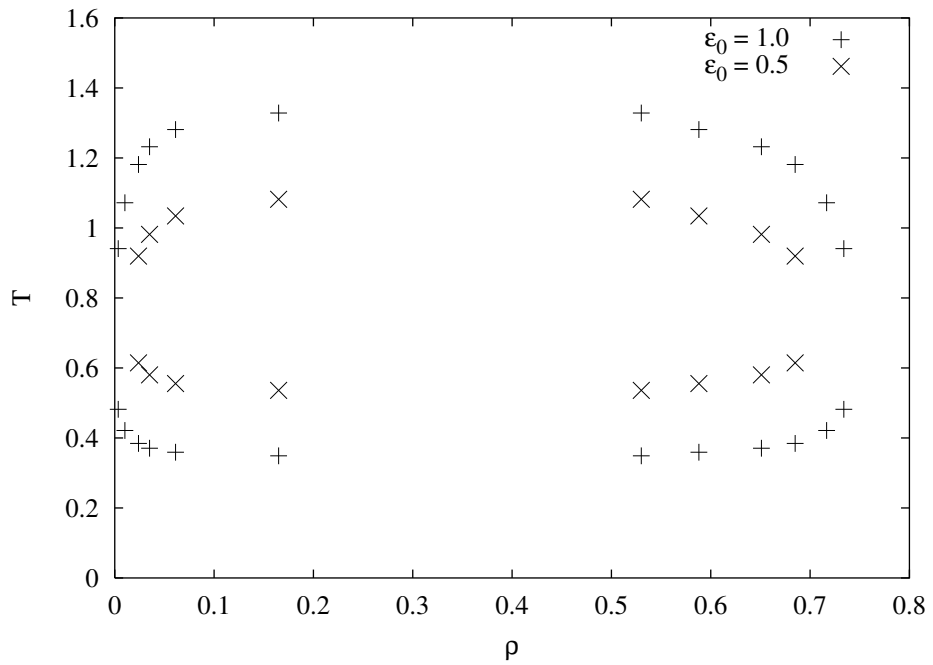


FIG. 5: Fluid-fluid coexistence curves for the two-dimensional square well model with solvent. The closed loop behavior is obtained using a simple model to illustrate the effects of temperature dependent parameters in the model on the fluid-fluid coexistence curve, as discussed in the text.

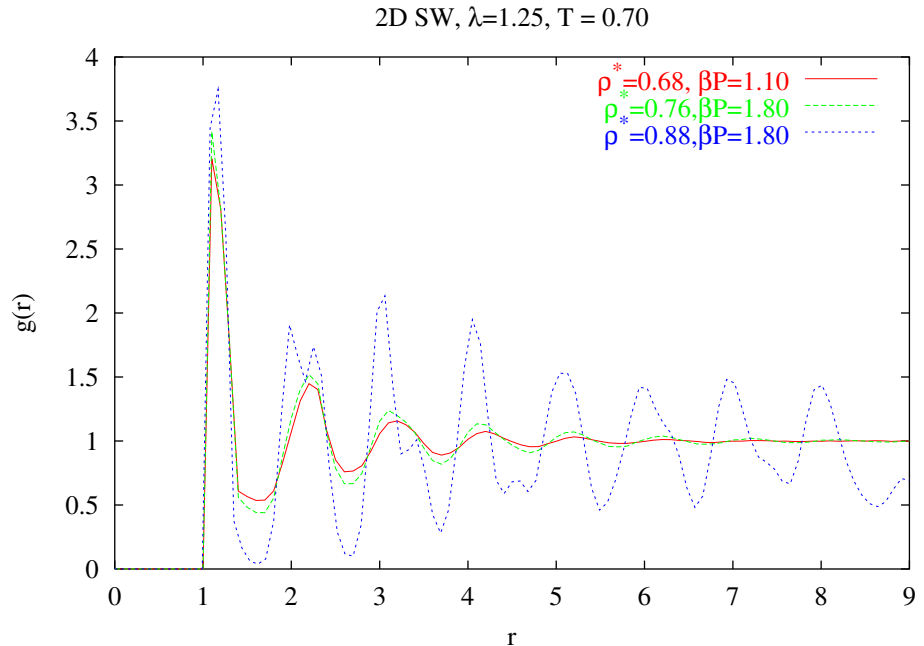


FIG. 6: Typical radial distribution functions for the liquid and solid phases at various densities  $\rho$  and pressures  $\beta P$ .

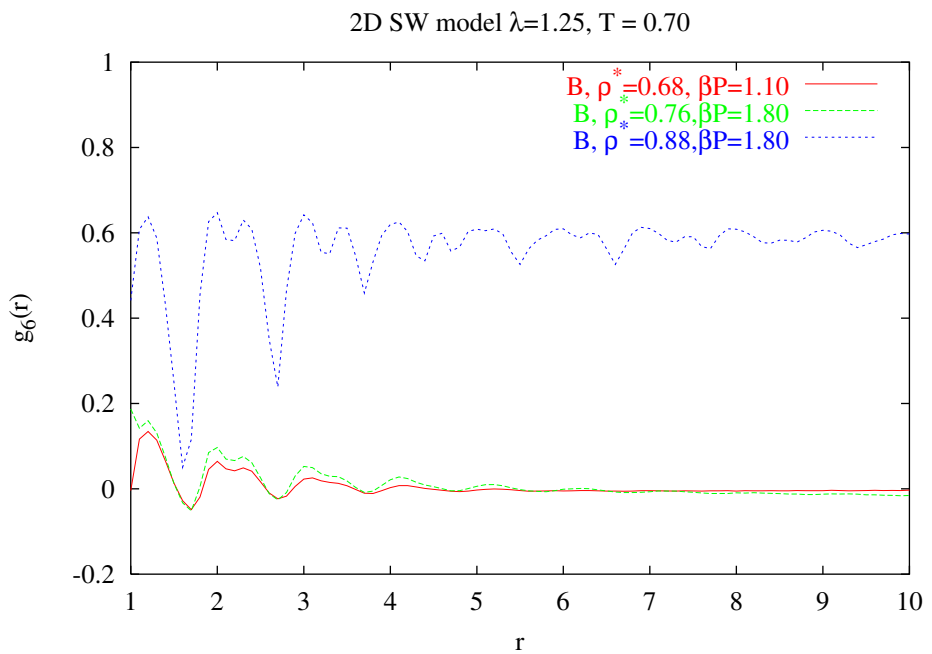


FIG. 7: Typical bond-order correlation functions for the liquid and solid phases at various densities  $\rho$  and pressures  $\beta P$ .

colloids) constrained to interact in quasi-two-dimensional space exhibit such phase diagrams. Figure 2 shows the fluid-fluid coexistence curves at the ranges we have studied, with solvent.

As discussed previously, many agents are added to a protein-solvent mixture to control the protein-protein interaction range. The second virial coefficient coefficient,  $B_2$ , is a measure of the net interaction and is commonly used as a means of determining the window for optimal globular protein crystallization<sup>20</sup>. This is presumably also true for membrane proteins. Therefore we show  $B_2/B_2^{HS}$  as a function of temperature in Figure 3. ( $B_2^{HS}$  is the second virial coefficient of hard spheres). In the absence of solute-solvent interactions,  $B_2 \rightarrow B_2^{HS}$  as  $T \rightarrow \infty$ , as the hard sphere interaction dominates. However, in the presence of solute-solvent interactions  $B_2 \rightarrow B_2^{HS}$  as  $T \rightarrow \frac{1}{3}$ . This occurs because where the effective interaction between particles  $\tilde{\epsilon}$  vanishes at that temperature, leaving only the hard sphere interaction. (The same situation occurs in three dimensions.) Although the second virial coefficient is only a function of temperature, if one plots its behavior along the coexistence curve, it becomes a function of density through the dependence of the coexistence temperature on density. We show this dependence in Figure 4. Along such a path the second virial coefficients with and without solvent-solute interaction are equal.

The model studied here can be also used to study the case in which the effective interactions introduced by the solute-solvent interaction are temperature-dependent. This can be obtained from eq. 4 by introducing temperature-dependent parameters  $\epsilon_w$  and  $\Delta s_w$ . To illustrate this situation, we use the four-level model of Muller, Lee, and Graziano<sup>21,22,23</sup> (MLG) for water, as it provides a simple example of such temperature dependent parameters. (We are not claiming that such a model is realistic in our case, but it does provide us with an illustrative example.) It can be shown<sup>15</sup> that  $\epsilon_w$  and  $\Delta s_w$  can be obtained in the MLG model as  $\epsilon_w(kT) = E_s - E_b$  and  $\Delta s_w(kT) = S_s - S_b$  where the former and latter equations are the differences in energy and entropy in the bulk and shell states, respectively. (See<sup>7</sup> for the definition of these energies and entropies.) Fig. 5 shows closed-loop fluid-fluid coexistence curves for choices of the parameter  $\epsilon_0 = 0.5$  and  $\epsilon_0 = 1.0$  in eq. 4.

Finally, we briefly discuss the possibility of a hexatic phase for our model. To test for this possibility, we determine the radial distribution function  $g(r)$  and the bond-order correlation function  $g_6(r)$  for the fluid and solid phases at  $\lambda = 1.25$ . Figures 6 and 7 show our results for typical values of pressure and temperature in the liquid and solid phases. Figure 6 shows two typical  $g(r)$  plots corresponding to a fluid phase as well as one corresponding to a solid

phase. Figure 7 shows our calculation of  $g_6(r)$ . For a hexatic phase, one would expect an algebraic decay. Our plot shows behavior typical of a fluid and solid;  $g_6(r)$  decays rapidly to zero in the fluid phase, indicating absence of long-range order, while that of the solid decays to a constant value. We see no evidence of a hexatic phase for our two dimensional model. However, as our system is quite small, finite size effects could be important. Therefore our results are certainly not definitive.

#### IV. CONCLUSION

We have studied the phase behavior of a simple model that is meant to describe the generic features of membrane proteins confined to a quasi-two-dimensional geometry. In particular, we have shown that a simple phenomenological model for the solute-solvent interactions can yield phase diagrams with upper and lower fluid-fluid critical points, as well as closed loops, depending on the choice of interaction parameters.

#### V. ACKNOWLEDGEMENTS

This work was supported by the G. Harold Mathers and Leila Y. Mathers Foundation and by the National Science Foundation, Grant DMR-0302598.

---

<sup>1</sup> H.M. Berman, J. Westbrook, Z. Feng, G. Gilliland, T.N. Bhat, H. Weissig, I.N. Shindyalov, P.E. Bourne, Nucleic Acids Research, **28** pp. 235-242 (2000)

<sup>2</sup> S.J. Singer and Garth L. Nicolson, Science **175**, 720 (1972)

<sup>3</sup> H. Michel, TIBS (February) p56 (1983)

<sup>4</sup> A. P. Gast, C. K. Hall, and W. B. Russel, J. Colloid Interface Sci., **96**, 251 (1983)

<sup>5</sup> H. N. W. Lekkerkerker et al., Eur ophys. Lett., **20**, 559 (1992); Tejero et al., Phys. Rev. Lett., **73**, 752 (1994)

<sup>6</sup> M. H. J. Hagen and D. Frenkel, J. Chem. Phys., **101**, 4093, (1994)

<sup>7</sup> D. Rosenbaum, P.C. Zamora, and C.F. Zukoski, Phys. Rev. Lett., **76**, 150 (1996)

<sup>8</sup> P. R. ten Wolde and D. Frenkel, Science, **277**, 1975 (1997)

<sup>9</sup> D. W. Oxtoby and V. Talanquer, J. Chem. Phys., **101**, 223 (1998)

<sup>10</sup> D.L. Pagan, M.E. Gracheva, and J.D. Gunton, *J. Chem. Phys.* **120**, 8292 (2004)

<sup>11</sup> A. Shiryayev and J.D. Gunton, *J. Chem. Phys.* **120**, 8398 (2004)

<sup>12</sup> D.L. Pagan and J.D. Gunton, *J. Chem. Phys.* **122**, 184515 (2005).

<sup>13</sup> M.A. Bates, M.G. Noro, and D. Frenkel, *J. Chem. Phys.* **116**, 7217 (2002)

<sup>14</sup> M.G. Noro and D. Frenkel, *J. Chem. Phys.* **114**, 2477 (2001)

<sup>15</sup> A. Shiryayev, D.L. Pagan, J.D. Gunton, D. Rhen, A. Saxena, and T. Lookman, *J. Chem. Phys.* **122**, 234911 (2005)

<sup>16</sup> A. Z. Panagiotopoulos, *Mol. Phys.* **61**, 813 (1987)

<sup>17</sup> D. Frenkel and B. Smit, *Understanding Molecular Simulation*, (San Diego, Academic Press 2002)

<sup>18</sup> P.J. Steinhardt, D.R. Nelson, and M. Ronchetti, *Phys. Rev. B* **28**, 784 (1983)

<sup>19</sup> L. Vega, E. de Miguel, L. F. Rull, G. Jackson and I. A. McLure, *J. Chem. Phys.* **96**, 2296 (1992)

<sup>20</sup> A. George and W. Wilson, *Acta Cryst. D* **50**, 361 (1994)

<sup>21</sup> N. Muller, *Acc. Chem. Res.* **23**, 23 (1990)

<sup>22</sup> B. Lee and G. Graziano, *J. Am. Chem. Soc.* **118**, 5163 (1996)

<sup>23</sup> S. Moelbert and P.D.L. Rios, *Macromolecules* **36**, 5845 (2003)